



The effects of $\text{Na}_2\text{O}/\text{SiO}_2$ molar ratio, curing temperature and age on compressive strength, morphology and microstructure of alkali-activated fly ash-based geopolymers

Alexandre Silva de Vargas^{a,*}, Denise C.C. Dal Molin^b, Antônio C.F. Vilela^c, Felipe José da Silva^d, Bruno Pavão^e, Hugo Veit^f

^a Materials Technology and Industrial Processes, Universidade Feevale, Novo Hamburgo, Brazil

^b Department of Civil Engineering, Universidade Federal do Rio Grande do Sul (UFRGS), Porto Alegre, Brazil

^c Department of Metallurgical Engineering, Universidade Federal do Rio Grande do Sul (UFRGS), Porto Alegre, Brazil

^d Instituto Militar de Engenharia (IME), Rio de Janeiro, Brazil

^e School of Civil Engineering, Universidade Federal do Rio Grande do Sul (UFRGS), Porto Alegre, Brazil

^f Universidade Federal do Rio Grande do Sul (UFRGS), Porto Alegre, Brazil

ARTICLE INFO

Article history:

Received 15 March 2009

Received in revised form 28 February 2011

Accepted 10 March 2011

Available online 21 March 2011

Keywords:

Fly ashes
Alkali activation
Residues
Geopolymers

ABSTRACT

Fly ashes (FA) are byproducts of electricity production from mineral coal in thermoelectric power plants. The pozzolanic properties of FA have been utilized in various applications, including structural concrete, yet the large part of FA is still discarded into the environment. To promote greater FA usage, this study aims to produce a dense matrix, with mechanical properties satisfactory for civil engineering projects, from alkali-activated fly ash-based geopolymers. Three variables were studied: the $\text{Na}_2\text{O}/\text{SiO}_2$ molar ratio (N/S 0.20, N/S 0.30 and N/S 0.40); curing temperature in the first 24 h (50, 65 and 80 °C); and age (1, 7, 28, 91 and 180 days). For this study, alkali-activated fly ash pastes and mortars were prepared. In pastes, morphology was studied using scanning electron microscopy (SEM/EDS) and microstructural properties with X-ray Diffraction (XRD) analysis. Mortars were evaluated according to their mechanical performance measured using compression strength tests. Compression strength results were analysed using ANOVA. The results show that the N/S molar ratio plays an important role in the mechanical and morphological characteristics of geopolymers. The mortars prepared with a N/S 0.40 molar ratio had the greatest compression strength. The analysis of paste morphology revealed that N/S 0.40 pastes had a denser appearance, which is in agreement with results of compression strength tests.

© 2011 Elsevier Ltd. All rights reserved.

1. Introduction

Fly ashes (FA) are byproducts of electricity generation in coal-fired power plants. FA are classified as cementitious ($\text{CaO} > 10\%$) and pozzolanic ($\text{CaO} < 10\%$) materials, and because of these properties, they are purchased by cement and concrete companies.

The southern region of Brazil has about 89% of the country's mineral coal reserves, which total about 28.8 billion tons. Estimates indicate that these reserves are enough to generate power for over one century [1]. Currently, coal-fired electrical power plants generate about 2 million tons of fly ashes in the region each year. Of this total, 20–30% is used by cement and concrete industries in the region, and the rest is disposed of in coal strip mining

trenches, which may cause extensive environmental damage, such as air, soil and groundwater contamination [2,3].

Alkali-activation is a technology that opens new paths for expanded use of several byproducts already traditionally used as mineral additives to cement, such as ground granulated blast furnace slag (GGBFS) from steel mills that use a blast furnace to produce pig iron [4–7], and fly ashes (FA) from coal-fired power plants [8–11].

According to Palomo et al. [12], the alkali-activation, often called geopolymerization, is a chemical process that changes vitreous structures (partially or fully amorphous and/or metastable) into well-compacted and cementitious composites. Van Jaarsveld et al. [13] added that polymerization requires a strongly alkaline medium to dissolve a certain amount of silica and alumina and to promote surface hydrolysis of the raw material particles. This medium can be obtained using simple or combined alkaline solutions, called activators. According to Roy [14], another feature of alkaline activators is that they stimulate the latent hydraulic properties of materials used in the process.

* Corresponding author. Tel.: +55 51 3586 8960; fax: +55 51 3586 8826.

E-mail addresses: alexandrev@feevale.br (A.S. de Vargas), dmolin@ufrgs.br (D.C.C. Dal Molin), vilela@ufrgs.br (A.C.F. Vilela), d4felipe@ime.eb.br (Felipe José da Silva), hugo.veit@ufrgs.br (H. Veit).

Hardjito and Rangan [15] have observed that geopolymers prepared with a 14 M solution of NaOH showed greater resistances to compression than the samples prepared with a 8 M solution of NaOH, regardless of curing temperature and age. Bakharev [25] and Hu et al. [16] have shown that the concentration of the NaOH solution plays the most important role in the strength of alkali-activated fly ash-based geopolymers. Palomo et al. [12], Silva and Thaumaturgo [17] and Komnitsas et al. [18] have also observed that the concentration of the activator has significant impact on the resistance to compression of geopolymers. However, they have found that there is an ideal concentration of the alkaline activator which contributes to increase the resistance of geopolymers. Beyond this ideal concentration, there could be loss of the material's mechanical properties, due to the presence of free OH^- in the alkali-activated matrix, which could change the material's geopolymer structure. Other variables that have significant impact on the mechanical properties of geopolymers are the curing temperature and age. However, the influence of these variables is only significant when the activator concentration is enough to drive the geopolymerization of aluminosilicates.

In that sense, this article aims to obtain a dense matrix, with mechanical properties satisfactory for civil engineering projects, from alkali-activated fly ash-based geopolymers. The studied process variables were the concentration of the NaOH solution, through $\text{Na}_2\text{O}/\text{SiO}_2$ molar ratio, the curing temperature in the first 24 h and age.

2. Experimental

2.1. Materials

Fly ash used in this study was generated in a coal-fired power plant located in southern Brazil. The fly ash used was Class F [19], had a low calcium content, was predominantly in the vitreous phase, and had some mullite, hematite and quartz crystalline inclusions (Fig. 1). The chemical composition of FA was determined using X-ray fluorescence spectrometry (Table 1). Mean ash particle diameter was $23.74\text{ }\mu\text{m}$ and surface area (Blaine) was $2700\text{ cm}^2/\text{g}$.

Fig. 2 shows the morphological appearances of FA particles in their original state. Numbers indicate sites where EDS analyses were conducted; results are shown in Table 2.

The alkaline activator used in this study was 97% sodium hydroxide (NaOH). The aggregate used was standard quartz sand at 4 granulations – 1.2, 0.6, 0.3 and 0.15 mm. Each represented 25% of the small aggregate used to prepare mortars (1:3, fly ash: aggregate), according to the NBR 7215 [20].

2.2. Methods

The methods used evaluated the effect of $\text{Na}_2\text{O}/\text{SiO}_2$ molar ratio (N/S 0.2, N/S 0.3 and N/S 0.4), curing temperature in the first 24 h (50, 65 and $80\text{ }^\circ\text{C}$), and age (1, 7, 28, 91 and 180 days) on the mechanical, morphological and microstructural properties of the alkaline-activated samples.

For this purpose, alkali-activated pastes and mortars were prepared. The pastes were prepared using the required water of normal consistency, according to NBR NM 43 [21]. When normal consistency was achieved, the samples were poured into 3.0-cm- and 5.0-cm-high plastic molds.

The mortars were prepared at 1:3 ratio (fly ash:sand; four different granulations), and the parameter was the consistency index of each mortar, established at $160 \pm 20\text{ mm}$. This index was adopted because it ensured that the material could condense easily in the 5.0-cm- and 10-cm-high cylindrical molds without exudation. Mortar was cast in the cylindrical molds according to NBR 7215 [20]: 4 layers and 30 pestle strokes applied to each layer. Compression strength of mortar samples for each age was calculated as the mean strength of four samples.

Pastes and mortar were cured at 50, 65 and $80\text{ }^\circ\text{C}$ for 24 h and then stored in a room at $24 \pm 1\text{ }^\circ\text{C}$ and 50% relative humidity until the different time points for morphological and microstructural analyses of pastes (1, 28 and 180 days) and measurement of mortar compression strength (1, 7, 28, 91 and 180 days). The surfaces of the molds with paste and mortar were covered with polyethylene film to simulate hydrothermal curing. According to Barbosa [22], this process avoids excessive water evaporation in alkali-activated

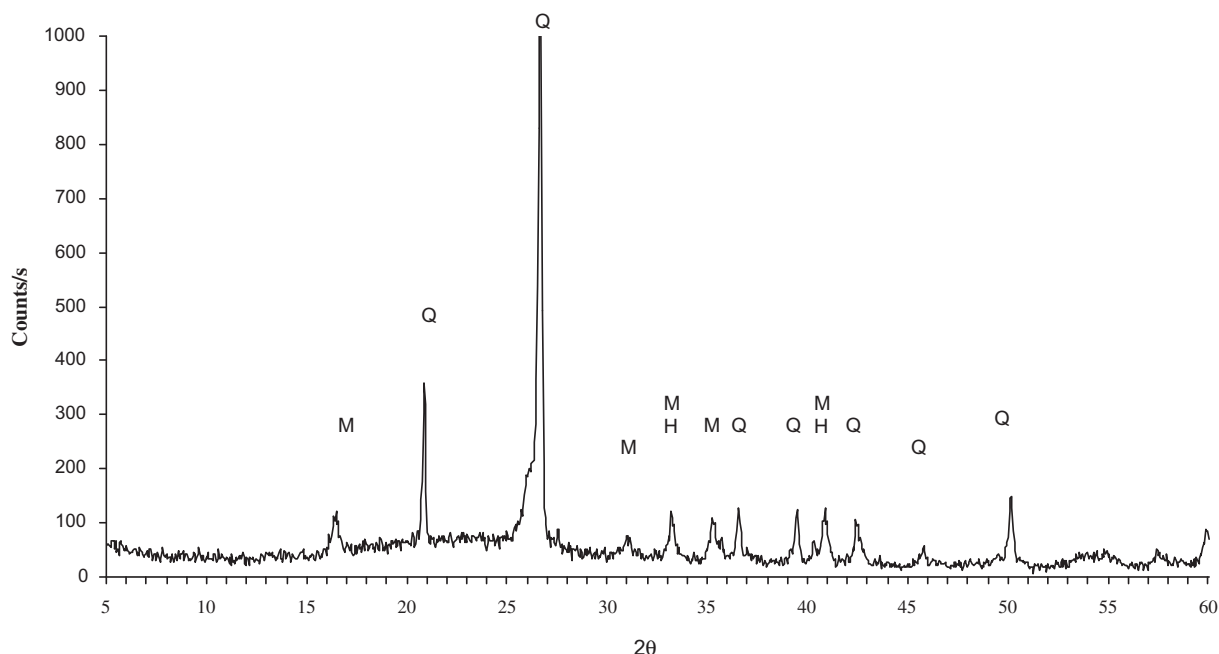
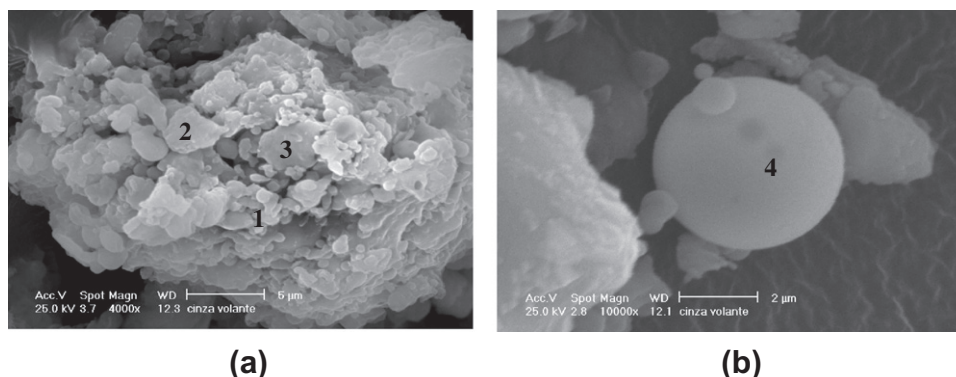


Fig. 1. XRD spectra of fly ash; Q = Quartz; M = Mullite; H = Hematite.

Table 1

Chemical composition of fly ash (% of mass).

SiO ₂	Al ₂ O ₃	CaO	Fe ₂ O ₃	Na ₂ O	TiO ₂	MgO	K ₂ O	SO ₄	I.R. ^a (%)	L.O.I. ^b (%)	Specific mass ^c (g/cm ³)
63.09	24.02	1.15	6.85	0.21	1.77	0.81	1.75	0.34	97.0	0.02	2.17

^a IR insoluble residue.^b L.O.I. loss on ignition.^c NBR NM 23 (ABNT, 2000).**Fig. 2.** Micrographs (secondary electron SEM) of fly ash in its original state: (a) spherical and non-spherical particle aggregates (4000×); (b) detail of fly ash spherical particle (10,000×). Numbers indicate sites where EDS analyses were conducted.**Table 2**

Semi-quantitative chemical analysis of fly ash determined by EDS; points of analysis are shown in Fig. 2a and b.

Point	Element					
	Content (%)					
	O	Al	Si	Ti	Fe	K
1	28.91	23.31	44.95	0.90	–	–
2	32.12	23.90	37.07	–	–	0.92
3	33.73	22.07	42.86	–	–	1.34
4	42.16	18.64	35.50	–	2.38	1.32

samples during thermal curing, an important step because water is necessary for polymerization.

Table 3 shows the molar compositions to obtain normal consistencies and to keep mortar consistency within the limits established in the study methods (160 ± 20 mm).

As the N/S values increased (greater NaOH concentration), the amounts of water (w/b and H/N) necessary to ensure that the pastes and mortars reach normal consistency and the reference consistency (160 ± 20 mm) decreased. This was associated with greater fly ash particle solubilization caused by the alkaline activator, which enabled the production of a greater amount of aluminosilicate gel. This gel was responsible for the greater workability of fresh samples and for mechanical strength when the material hardened.

Table 3

Molar composition to obtain alkali-activated fly-ash pastes and mortars using NaOH solution.

Pastes and mortar		Pastes ^a		Mortars ^b		
N/S	S/A	H/N	w/b	H/N	w/b	Consistency (mm)
0.20	4.45	16.07	0.550	18.11	0.622	174
0.30		10.34	0.502	11.64	0.566	171
0.40		7.47	0.458	8.51	0.522	165

N = Na₂O; S = SiO₂; A = Al₂O₃; H = H₂O; w/b - water/binder ratio.^a Necessary ratios to obtain normal consistency.^b Necessary ratios to ensure that mortar consistency index was within the limits established in the study methods (160 mm ± 20 mm).

3. Results and analysis

3.1. Compression strength

Mean compression strength values for the N/A 0.20, 0.30 and 0.40 samples cured at 50, 65 and 80 °C in the first 24 h at different ages are shown in Table 4.

Table 5 summarizes the results of ANOVA to evaluate the effect of N/S molar ratio, curing temperature, age and the interaction of these variables in the results of compression strength of alkali-activated samples. The level of significance was set at 95%. ANOVA results revealed that N/S molar ratio, curing temperature and age, as well as the interaction of these variables, had a significant effect on the results of compression strength of the alkali-activated samples (Fig. 3).

At age 1 day, strength values were relatively low (between 1 and 4 MPa). From 7 days on, the mechanical performance of N/S 0.3 and N/S 0.4 samples is different from that of N/S 0.2 samples. Results increased for the N/S 0.3 and N/S 0.4 samples up to 91 and 180 days, respectively. For the N/S 0.20 samples, mechanical results changed very little along time. These results indicate that fly ash samples prepared with low NaOH concentrations (N/S 0.20) do not have a satisfactory mechanical performance, as strength values of about 2 MPa for a binder are not useful in civil engineering. In this case, variables such as curing temperature and age did not significantly affect the gain in compression

Table 4

Mean compression strength values for the alkali-activated fly ash mortars prepared using different molar ratios and cured at one of three different temperatures in the first 24 h at different ages.

Age (days)	Mean compression strength (MPa)								
	N/S molar ratio								
	0.20			0.30			0.40		
	Curing temperature (°C)								
	50	65	80	50	65	80	50	65	80
1	0.74	0.64	0.89	2.20	1.78	3.61	0.90	1.18	2.69
7	1.76	1.59	1.31	3.01	3.63	5.53	2.40	3.15	5.25
28	2.18	1.76	1.79	9.22	8.99	11.85	8.94	9.57	13.74
91	2.20	2.06	2.23	12.41	11.67	14.30	16.26	15.32	17.69
180	2.39	1.94	1.48	12.52	12.08	14.91	19.34	19.38	21.28

Table 5

Analysis of variance (ANOVA) of the effect of N/S molar ratio, curing temperature, age and the interaction of these variables on compression strength of the alkali-activated samples.

Factor	Df	QM	CalF	F0.05	Significance ^a
N/S ratio	2	818.42	3979.8	3.10	S
Temperature	2	33.29	161.91	3.10	S
Age	4	463.86	2255.64	2.47	S
N/S ratio ^a temperature	4	9.80	47.67	2.47	S
N/S ratio ^a age	8	109.25	531.27	2.04	S
Temperature ^a age	8	1.01	4.95	2.04	S
N/S ratio ^a temperature ^a age	16	0.62	3.03	1.76	S
Error	87	0.206			

Df: Degree of freedom, S: Significant, QM: Quadratic mean, NS: Not significant, CalF: Calculated value of F, F0.05: Table value for F at a level of significance of 95%.

^a Significance: CalF > F0.05 = S, CalF < F0.05 = NS.

strength of the N/S 0.20 mortars. The low mechanical performance of these mortars was due to insufficient attack to FA and, consequently, inadequate FA solubilization and formation of an

insufficient amount of aluminosilicate gel. This finding will be evaluated in the microstructural description of the alkali-activated pastes, as shown in Fig. 5.

At the same time, there was greater interaction between NaOH and FA for the N/S molar ratio of 0.40 at later ages (91 an 180 days) (Fig. 3). This means that age will more effectively affect the gain in compression strength of samples that have higher N/S ratios. In this case, it was from 28 days on that the mechanical performance of the N/S 0.40 samples stood out when compared to N/S 0.30 samples. For example, between 28 and 180 days, the significant mean increase in strength values of N/S 0.40 samples cured at 80 °C/24 h was 55%, whereas the N/S 0.30 samples, cured at the same temperature, had an increase of 25%.

The FA is composed of perlospheres, inside which the microspheres are found. To ensure that the alkaline activator comes in contact with the microspheres, and that polycondensation occurs, it is first necessary to break the perlospheres, as can be seen in Fig. 4 [23]. The alkaline activator reached the cenospheres only after the partial dissolution of the external layer of the perlosphere, which demonstrates that the polymerization of the perlosphere

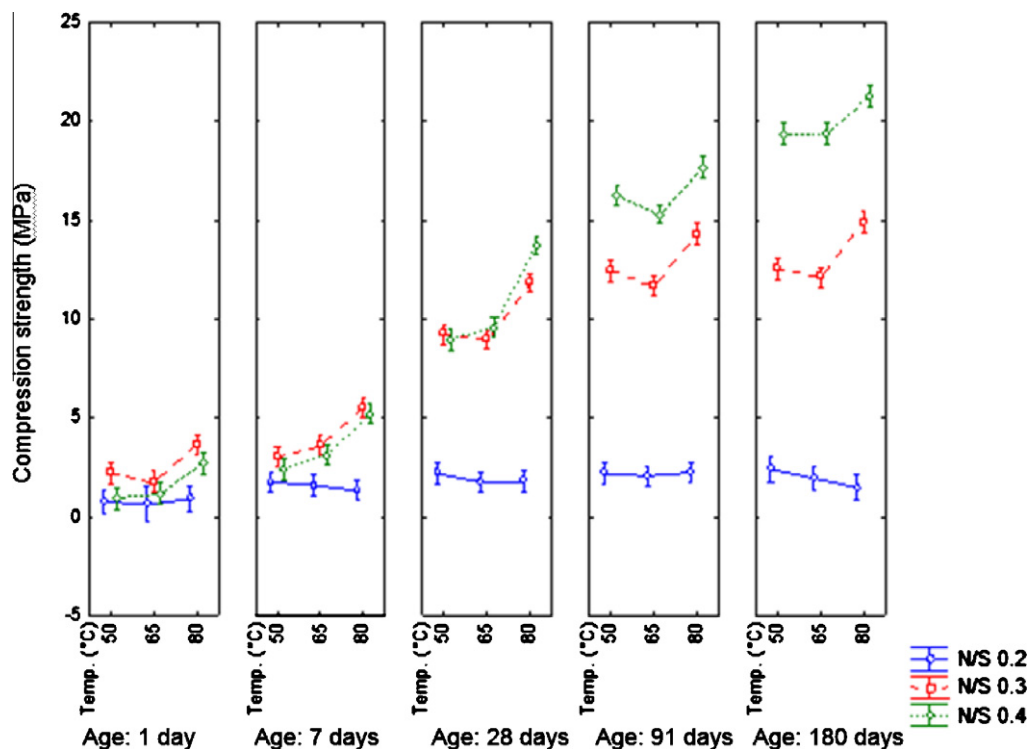


Fig. 3. Effect of interaction between age, curing temperature and $\text{Na}_2\text{O}/\text{SiO}_2$ (N/S) molar ratio in compression strength (MPa) of the alkali-activated mortars.

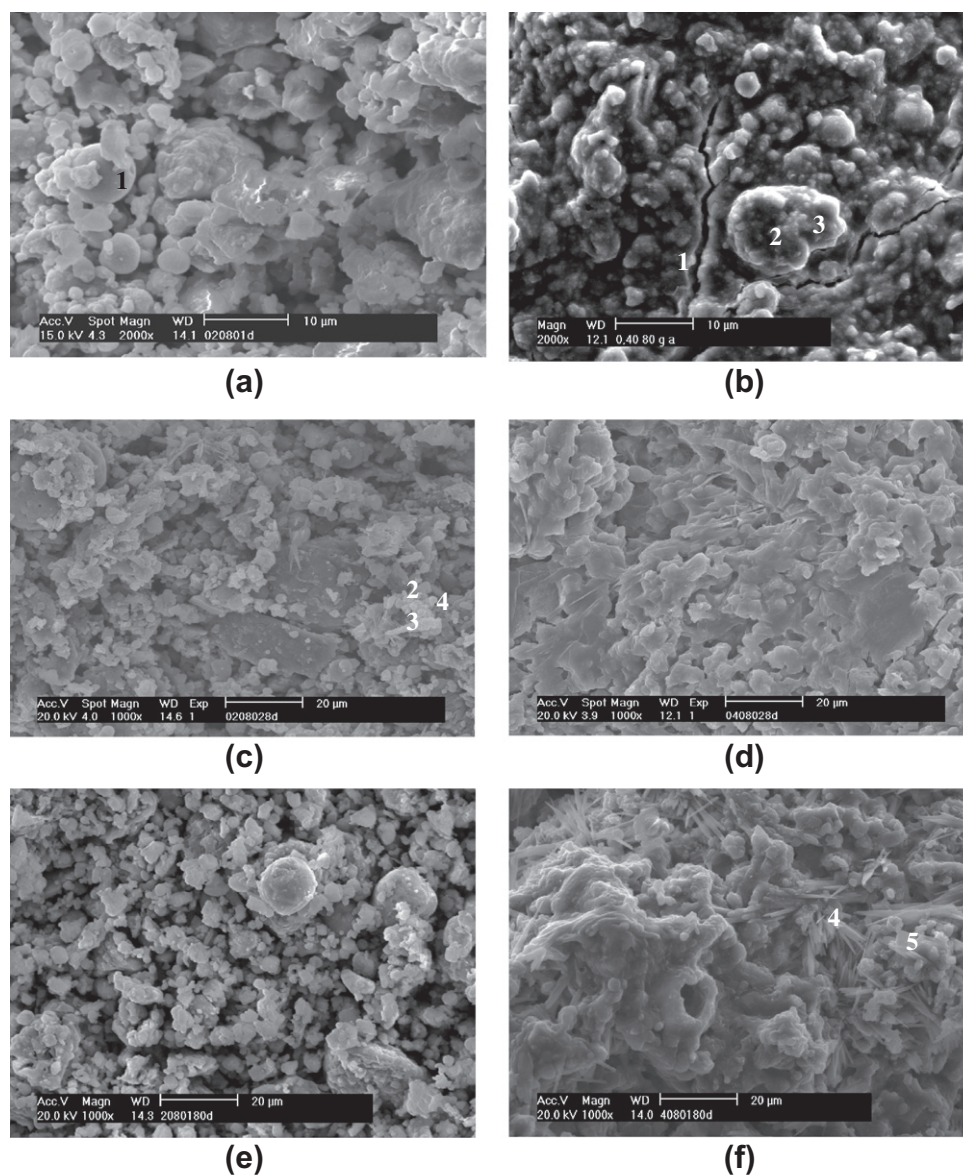


Fig. 5. Micrographs (SEM) of N/S 0.20 paste cured at 80 °C/24 h at: (a) 1 day; (c) 28 days; (e) 180 days. Micrographs (SEM) of N/S 0.40 paste cured at 80 °C/24 h at: (b) 1 day; (d) 28 days; (f) 180 days. Images (a) and (b) magnified to 2000 \times ; (c), (d), (e) and (f) to 1000 \times . Numbers in figures indicate EDS images.

structures occurs from the outside to the inside, where the microspheres are attacked. These findings are in agreement with the model of FA alkali-activation described by Fernández-Jiménez et al. [11].

This explains the gain in strength that is seen along time in the alkali-activated samples, particularly between 7 and 28 days. The reaction of these microspheres generated extra reaction products, which packed up the microstructure and generated a significant increase in strength of about 161% in this time interval for the N/S 4.0 samples cured at 80 °C/24 h.

Still according to Fig. 3, curing temperatures affected compression strengths of N/S 0.30 and N/S 0.40 samples. Regardless of age, samples cured at 80 °C/24 h had the best compression strength results. Therefore, high curing temperatures resulted in a more efficient alkaline attack to FA. However, at later ages, there was a reduction in the difference in mean compression strength values between samples cured at 80 °C/24 h and those cured at lower temperatures (50 or 65 °C). For example, at 1, 28 and 180 days, the difference in mean compression strength between N/S

0.40 samples cured at 50 °C and N/S 0.40 cured at 80 °C was 198% (0.90 MPa and 2.69 MPa), 54% (8.94 MPa and 13.74 MPa) and 10% (19.34 MPa and 21.28 MPa), respectively. Therefore, temperature increases are important for faster gain in strength when the goal is higher strengths in short periods of time.

The Fisher analysis of the results of N/S 0.30 and N/S 0.40 samples did not reveal any significant increase in compression strength when curing temperature increased from 50 to 65 °C. This can be seen in Fig. 3, in which the results of compression strength are very close and always within the limits of the error bar, regardless of age. There was no unusual gain in strength for the samples cured at these temperatures. Temperature, therefore, had a significant effect on the N/S 0.30 and N/S 0.40 samples only at 80 °C in this study.

Based on the explanations above, we concluded that age, curing temperature and N/S molar ratio are the variables that significantly affected compression strength of the alkali-activated samples only for those samples in which aluminosilicate gel formation was effectively found (N/S 0.30 and N/S 0.40 samples). We also found

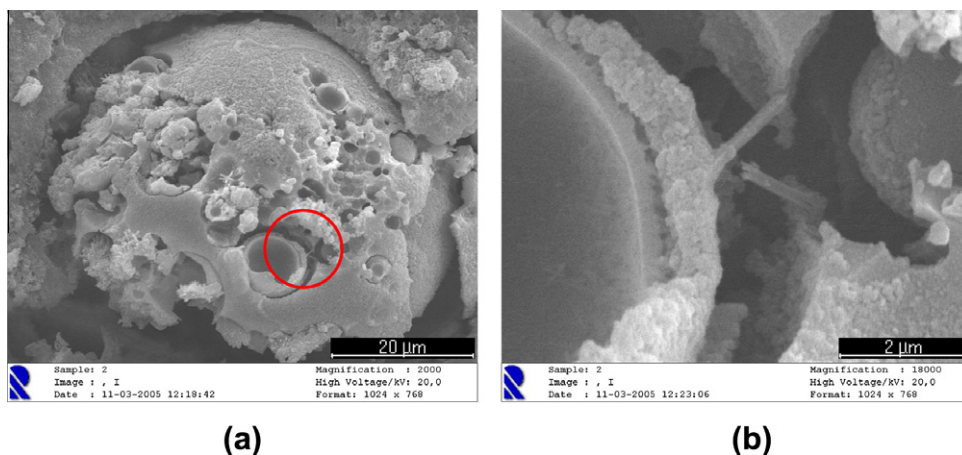


Fig. 4. Morphological appearance of an alkali-activated fly ash paste at 28 days; (a) partially solubilized plerospheres, and a view of microspheres inside them; (b) appearance of the external layer of the microsphere attacked by the alkaline activator. Region highlighted in Fig. 4a.

that there was a strong association between these variables, particularly between age and N/S molar ratio. For those samples in which aluminosilicate gel formation was deficient (N/S 0.20) or even absent, temperature and age were not important in the alkali-activation technology.

Therefore, the best mechanical performance was found for the N/S 0.40 alkali-activated samples cured at 80 °C/24 h at 180 days.

The conditions described are not necessarily ideal for other studies that may use alkali-activation because variables, such as raw materials, curing conditions, age (curing time), type and concentration of activator, will significantly affect the physical and mechanical properties of the end product. In addition, these variables are interdependent, which may make both performance and control more difficult.

3.2. Phase composition of fly ash pastes

Fig. 5a, c and e shows micrographs of the fracture surface of N/S 0.20 pastes cured at 80 °C/24 h at 1, 28 and 180 days. The analysis of the morphology of the paste revealed that, in general, the matrix contains only aggregated and practically intact FA particles after their contact with the alkaline activator even at 180 days. This demonstrates that a molar ratio of N/S 0.20 was not enough to produce an attack to FA particles, which prevented the production of aluminosilicate gel. The microstructural behavior of the matrix of the N/S 0.20 sample, regardless of curing temperature and age, is in agreement with its macrostructural behavior (compression strength) shown in Fig. 3. There was no significant gain in strength when age and curing temperature changed. Such results indicate that these variables become unimportant when the alkaline activator concentration is not high enough to cause the solubilization of fly ash particles and, later, the formation of aluminosilicate gel. Crystalline formations were found in the alkali-activated paste at 28 days, as shown in Fig. 5c.

Table 6 shows EDS results and EDS points of analysis are shown in Fig. 5a and c. Point 1 indicates the chemical analysis of an FA particle (Fig. 5a), which contains 3.42% Na and an Si/Al atomic ratio of 1.27. This value is close to the interval calculated for the Si/Al ratio obtained with the original FA (1.30–1.55; Table 2), which confirmed the low dissolution of this paste when the N/S 0.20 molar ratio was used.

At points 2, 3 and 4, Na contents were greater than the value found in point 1. The sodium aluminosilicate phases formed at these points, and this indicates that alkali-activation took place at different points of the matrix. It is not ruled out, however, that these formations might indicate the presence of carbonates. These

Table 6

EDS (semi-quantitative) chemical analysis of N/S 0.20 paste cured at 80 °C/24 h at 1 and 28 days. Points of analysis are shown in Fig. 5a and c.

Point	Figure	Element			
		Content (%)			
		O	Na	Al	Si
1	5a	32.13	3.42	27.68	36.78
2	5c	28.08	16.01	17.41	38.51
3		42.70	15.53	15.27	26.50
4		38.35	13.29	15.00	33.35

compounds may coexist in the same region around an attacked particle, as might be the case of the particle shown in Fig. 5c. The formation of carbonates in these matrices was confirmed also using XRD analysis (Fig. 6).

Therefore, the N/S 0.20 molar ratio was not ideal for the alkali-activation of fly ashes used in this study, regardless of the curing temperature and age, because our purpose was to obtain a dense matrix with mechanical properties satisfactory for civil engineering.

Fig. 5b, d and f shows the characteristic microstructures of the N/S 0.40 paste cured at 80 °C/24 h at 1, 28 and 180 days. Table 7 shows the results of the EDS semi-quantitative chemical analysis of this sample at 1 and 180 days.

The microstructure of the N/S 0.40 sample at 1 day had a high degree of solubilization of FA particles, but also multiple microfissures. The EDS results in Table 7 show that the region in which a larger number of FA particles were seen had a Si/Al atomic ratio close to 1.41 (points 2 and 3, Fig. 5b), and the one that was more solubilized had a value of 2.31 (point 1, Fig. 5b).

Fig. 5f shows the formation of the Na-rich crystalline phase in the 180-day-old sample, according to the chemical analysis in Table 7. XRD results, presented in this study, revealed the formation of carbonated compounds.

These carbonate phases did not affect the mechanical performance of mortars negatively. On the contrary, a significant gain in compression strength of about 55% was found at 28 and 180 days.

Therefore, age was associated with visible changes in the microstructure of the N/S 0.40 sample, and crystalline compounds formed along time. Moreover, microfissures were usually seen in the alkali-activated matrices. A similar behavior was reported by Fernández-Jiménez et al. [24] in a study with AAFA pastes. According to those authors, the origin of microfissures might be associ-

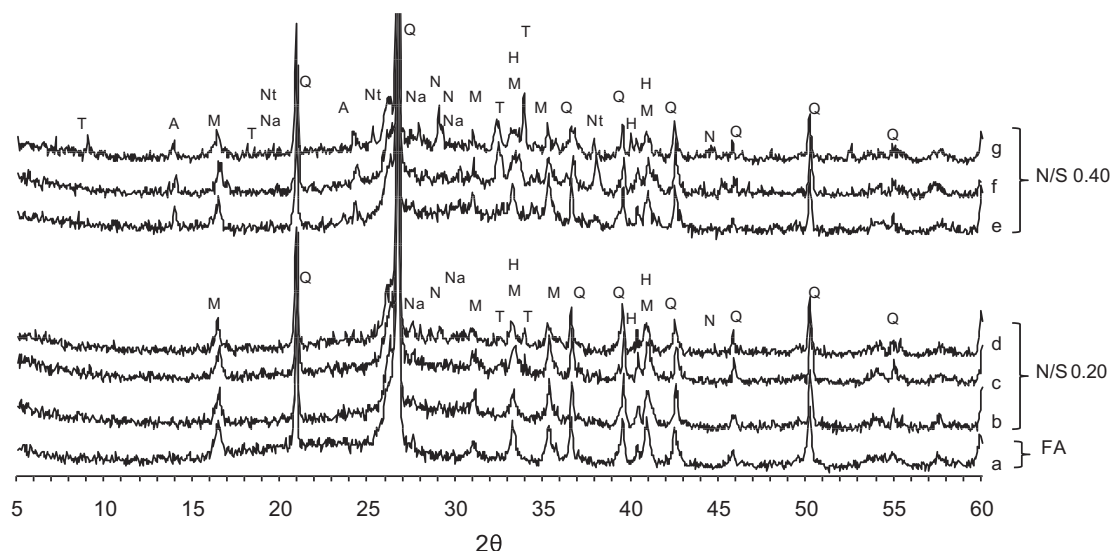


Fig. 6. XRD spectra (a) un-reacted fly ash; N/S 0.20 24 h at 80 °C (b) 1 day, (c) 28 days, (d) 180 days; N/S 0.40 24 h at 80 °C (e) 1 day, (f) 28 days, (g) 180 days; Q = Quartz; M = Mullite; H = Hematite; N = Nacrolite; Na = Natrite; T = Trona; A = albite; Nt = Natron.

Table 7

EDS semi-quantitative chemical analysis of alkali-activated fly ash paste at 1 and 180 days: N/S 0.40 cured at 80 °C/24. Points of analysis are shown in Figs. 5b and f.

Point	Figure	Element (%)			
		O	Na	Al	Si
1	5b	47.96	10.65	12.13	29.26
2	5b	34.98	7.23	23.54	34.25
3	5b	39.13	10.87	20.01	29.98
4	5f	24.50	18.47	23.59	33.45
5	5f	30.28	28.77	15.92	25.03

ated with some factors, such as: thermal curing; retraction due to vacuum drying in SEM; or even the interaction between these two variables. Silva and Thaumaturgo [17] also found that alkali-activated GGBFS/MK-based pastes had microfissures in the matrix, similarly to those seen in alkali-activated fly ash (AAFA) pastes. According to those authors, the addition of mineral fillers or fibers substantially improved the physical and mechanical properties of the composite.

Microfissures were more easily detected in the samples with greater solubilization (N/S 0.40 samples) than in the samples in which FA dissolution was partial (N/S 0.20 samples). Although microfissures were found in the alkali-activated matrix, together with the formation of crystalline compounds, there was no reduction in compression strength along time.

3.3. XRD

Fig. 6 shows the XRD spectra of un-reacted fly ash (a) and alkali-activated pastes prepared with N/S 0.20 and N/S 0.40 molar ratio, cured at a temperature of 80 °C/24 h, and analysed at 1, 28 and 180 days.

The spectra of N/S 0.40 samples at 1 day (e) showed crystalline peaks characteristics of nahcolite (NaHCO_3), natrite (Na_2CO_3) and albite ($\text{NaAlSi}_3\text{O}_8$). A comparison with spectra of N/S 0.20 samples at 1 day (b) revealed that there was an effect on the rate of reactions of the alkali-activated pastes with the increase of the molar ratio, and only the trona phase was detected at 1 day for the N/S 0.20 samples.

As the age of N/S 0.40 samples increased, new crystalline phases formed. For example, at 28 days (f), trona was detected

($\text{Na}_3\text{H}(\text{CO}_3)_2 \cdot 2\text{H}_2\text{O}$), and at 180 days (g), natron ($\text{Na}_2\text{CO}_3 \cdot \text{H}_2\text{O}$). These results are in agreement with SEM/EDS micrographs (Fig. 5f) which found acicular crystalline formations in N/S 0.40 samples.

The original FA (a) crystalline peaks of quartz, mullite and hematite were also found in the N/S 0.40 samples. However, these peaks tended to lose intensity along time. This finding apparently suggests that reactions disorganized the structure of the crystalline phases of the FA particles (quartz, mullite and hematite) produced by the alkaline activator as the age of the activated pastes increased. This behavior was not observed in the spectra of the N/S 0.20 samples. As described, there was not enough solubilization of the FA particles in these samples.

However, in addition to changing the reaction velocity with the increase of the alkaline activator (NaOH) concentration, there was also an increase in the number of crystalline compounds at 1 day in the N/S 0.40 samples, which demonstrated an effect on the formation of new crystalline compounds (albite and natron) in these samples, not detected in the N/S 0.20 samples.

The detection of crystalline compounds in the AAFA samples, particularly those common to FA (quartz, mullite and hematite) is in agreement with the results reported by Bakharev [25], Fernández-Jiménez et al. [26], and Criado et al. [27] in AAFA pastes.

4. Conclusions

This study has shown that the N/S molar ratio played the most important role in resistance to compression, in the morphology and microstructure of alkali-activated fly ash-based geopolymers. Temperature and age only affected the gain in strength in alkali-activated fly ash samples when there was formation of aluminosilicate gel in the alkali-activated matrix. The N/S 0.40 molar ratio sample was the one that yielded the greatest compression strength for mortars and denser morphology in geopolymer pastes.

As the N/S molar ratio increased (greater concentration of NaOH), the amounts of water necessary to ensure that the pastes and mortars reach normal consistency and the reference consistency decreased. This was associated with greater fly ash particle solubilization caused by the alkaline activator, which enabled the production of a greater amount of aluminosilicate gel. This gel was responsible for the greater workability of fresh samples and for mechanical strength when the material hardened.

The XRD spectra revealed original crystalline phases of fly ash – quartz, mullite and hematite – and crystalline phases containing CO_2 and Na in all samples, regardless of the other variables under study. However, a trend towards intensity reduction of the crystalline peaks of quartz, mullite and hematite was observed at later ages for the N/S 0.40 samples. Apparently, some reactions promote a structural disorganization of the crystalline phases of the FA particles in consequence of the alkaline medium produced by the NaOH activator.

References

- [1] Vieira JC. Valorização do “Ouro Negro”. *Jornal Correio do Povo* 2005; Porto Alegre (brazil) no 312, 4 agosto; 2005. p. 4 [in Portuguese].
- [2] Rohde GM. Cinzas de carvão no Brasil: Restrições ambientais e medidas mitigadoras. In: Rohde GM, et al. Cinzas de carvão fóssil no Brasil – Aspectos Técnicos e Ambientais, Porto Alegre: CIENTEC. 2006. p. 137–95 [chapter 2, in Portuguese].
- [3] Vargas AS. Cinzas volantes álcali-ativadas para a obtenção de aglomerantes especiais. Porto Alegre. Tese (Doutorado em Engenharia) – Curso de Pós-Graduação em Engenharia de Minas, Materiais e Metalurgia (PPGEM), UFRGS. 2006. p. 169 [in Portuguese].
- [4] Puertas F, Fernández-Jiménez A. Mineralogical and microstructural characterisation of alkali-activated fly ash/slag pastes. *Cem Concr Compos* 2003;25:287–92.
- [5] Deja J. Properties of activated pastes containing metakaolin and other mineral additives. In: of The 11th international congress on the chemistry of cement (ICCC), 11, Africa of South; 2003. p. 832–42.
- [6] Fernández-Jiménez A, Palomo JG, Puertas F. Alkali-activated slag mortars mechanical strength behaviour. *Cem Concr Res* 1999;29:1313–21.
- [7] John V M. Cimentos de escória ativada com silicatos de sódio. São Paulo. Tese (Doutorado em Engenharia) – Departamento de Engenharia de Construção Civil, Escola Politécnica da Universidade de São Paulo (EPUSP); 1995. p. 200 [in Portuguese].
- [8] Skavara F, Slosar J, Bohunck J, Markova A. Alkali-activated fly ash geopolymeric materials. In: Of the 11th international congress on the chemistry of cement (ICCC), 11, Africa of South; 2003. p. 1341–1350.
- [9] Sofi M, Van Deventer JSJ, Mendis PA, Lukey GC. Engineering properties of inorganic polymer concretes (IPCs). *Cement Concrete Res* 2007;37:251–7.
- [10] Katz A. Microscopic study of alkali-activated fly ash. *Cement Concrete Res* 1998;28(2):197–208.
- [11] Fernández-Jiménez A, Palomo A, Criado M. Microstructure development of alkali-activated by fly ash cement: a descriptive model. *Cement Concrete Res* 2005;35:1204–9.
- [12] Palomo A, Grutzeck MW, Blanco MT. Alkali-activated fly ashes. a cement for future. *Cement Concrete Res* 1999;29:1323–9.
- [13] Van Jaarsveld JGS, Van Deventer JSJ, Lorenzen L. The potential use of geopolymeric materials to immobilise toxic metals: Part I. Theory and applications. *Miner Eng* 1997;10(7):659–69.
- [14] Roy DM. Alkali-activated cements opportunities and challenges. *Cement Concrete Res* 1999;29:249–54.
- [15] Hardjito D, Rangan BV. Development and properties of low-calcium fly ash-based geopolymer concrete. In: Research report GC, 1, Australia 2005. Perth. Faculty of Engineering Curtin University of Technology; 2005. p. 1–94.
- [16] Hu M, Zhu X, Long F. Alkali-activated fly ash-based geopolymers with zeolite or bentonite as additives. *Cem Concr Compos* 2009;31(10):762–8.
- [17] Silva FJ, Thaumaturgo C. Use of environmental scanning electron microscopy (ESEM) to study Alkali-activated pulverized fly-ash. In: The Brazilian conference on microscopy of materials, MICROMAT 98 – ACTA MICROSCÓPICA, 6, Água de Lindóia, São Paulo (Brazil); 1998. p. 133–136.
- [18] Komnitsas K, Zaharaki D, Perdikatsis V. Effect of synthesis parameters on the compressive strength of low-calcium ferronickel slag inorganic polymers. *J Hazard Mater* 2009;161:760–8.
- [19] American Society for testing and materials (ASTM). Standard specification for coal fly ash raw or calcined original pozzolan for use as a mineral admixture in concrete. ASTM C618/98. In: Annual book of ASTM, V. 04.02, Philadelphia; 1998.
- [20] Associação brasileira de normas técnicas. NBR 7215: cimento Portland – determinação da resistência à compressão, Rio de Janeiro; 1996 [in Portuguese].
- [21] Associação brasileira de normas técnicas. NBR MN 43: cimento Portland – determinação da pasta de consistência normal, Rio de Janeiro; 2003 [in Portuguese].
- [22] Barbosa VFF. Síntese e caracterização de Polissialatos. Rio de Janeiro, Tese (Doutorado em Engenharia) – Departamento de Ciências dos Materiais, Instituto Militar de Engenharia (IME); 1999. p. 199 [in Portuguese].
- [23] Vargas AS, Dal Molin DCC, Vilela Said J, Castro-Gomes JP. Cinzas volantes álcali-ativadas com solução combinada de NaOH e Ca(OH)_2 . *Rev Matéria* 2007;12(3):462–9.
- [24] Fernández-Jiménez A, Palomo A. Alkali-activated fly ash concrete: alternative material for the precast industry. In: seminário geopolímeros – desenvolvimento recentes e suas aplicações na engenharia, I. Vila Real, Portugal; 2004. p. 1–16.
- [25] Bakharev T. Geopolymeric materials prepared using class F fly ash elevated temperature curing. *Cem Concr Res* 2005;35:1224–32.
- [26] Fernández-Jiménez A, Palomo A. Composition and microstructure of alkali activated fly ash binder: effect of the activator. *Cem Concr Res* 2005;35(10):1984–92.
- [27] Criado M, Fernández-Jiménez A, De La Torre AG, Aranda MAG, Palomo A. An XRD study of the effect of the $\text{SiO}_2/\text{Na}_2\text{O}$ ratio on the alkali activation of fly ash. *Cement Concrete Res* 2007;37:671–9.